

RESEARCH COMMUNICATIONS

16. Trong Thi Mai, Fu-Li Hsiao, Chengkuo Lee, Wenfeng Xiang, Chii-Chang Chen and Choi, W. K., Optimization and comparison of photonic crystal resonators for silicon microcantilever sensors. *Sensors Actuat. A*, 2011, **165**, 16–25.
17. Li, B., Hsiao, F. L. and Lee, C., Configuration analysis of sensing element for photonic crystal based NEMS cantilever using dual nano-ring resonator. *Sensors Actuator. A: Phys.*, 2011, **169**, 352–361.
18. Li, B., Fu-Li Hsiao and Chengkuo Lee, Computational characterization of a photonic crystal cantilever sensor using a hexagonal dual nano ring based channel drop filter. *IEEE Trans. Nanotechnol.*, 2011, **10**(4).
19. Yi Yang, Daquan Yang, Huiping Tian and Yuefeng Ji, Photonic crystal stress sensor with high sensitivity in double directions based on shoulder-coupled aslant nano cavity. *Sensors Actuat. A*, 2013, **193**, 149–154.

Received 20 October 2015; revised accepted 26 December 2015

doi: 10.18520/cs/v110/i10/1989-1994

Study of relationship between daily maxima in ozone and temperature in an urban site in India

S. S. Gunthe¹, G. Beig² and L. K. Sahu^{3,*}

¹EWRE Division, Department of Civil Engineering, Indian Institute of Technology Madras, Chennai 600 036, India

²Indian Institute of Tropical Meteorology, Pashan, Pune 411 008, India

³Physical Research Laboratory, Navarangpura, Ahmedabad 380 009, India

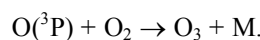
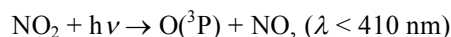
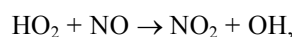
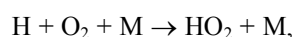
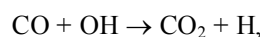
The relationship between surface-level observations of daily maxima in ozone ($O_{3\max}$) volume mixing ratio and ambient air temperature (T_{\max}) has been studied at an urban site, i.e. Pune (18.4°N, 73.8°E), India during 2003–04. The mixing ratios of $O_{3\max}$ were found to be highest during winter to pre-monsoon period and lowest in the monsoon season. The dependence of $O_{3\max}$ levels on T_{\max} has been quantified using the linear regression fit for the different seasons. However, except for the monsoon season, reasonably good correlations between $O_{3\max}$ and T_{\max} were noticed. The correlation between daily $O_{3\max}$ concentration and minimum NO_x ($NO_{x\min}$) concentration was also studied to assess the importance of photochemical mechanism mainly reduction in the loss due to titration. Overall, the strong dependencies of $O_{3\max}$ on T_{\max} and $NO_{x\min}$ signify the role of both meteorological and photochemical processes during most months of a year. The positive slopes of $\Delta O_{3\max}/\Delta T_{\max}$ and $\Delta O_{3\max}/\Delta NO_{x\min}$ clearly indicate the role of significant production and accumulation of O_3 under high temperature and low NO_x conditions respectively, during winter and pre-

monsoon seasons. The statistical analysis of O_3 in relation with the key meteorological and chemical parameters is important to understand the sensitivity of secondary pollutants on various controlling factors.

Keywords: Air temperature, ozone, precursors, seasonal variations.

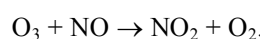
It is well known that surface level ozone (O_3) is one of the important photochemical pollutants due to its strong oxidizing nature. Ozone is produced by the photo-oxidation of precursor gases like volatile organic compounds (VOCs), carbon monoxide (CO) and nitrogen oxides (NO_x ; i.e. $NO + NO_2$) in the presence of sunlight¹. For example, the following set of reactions initiated by the oxidation of CO shows the mechanism of photochemical production of O_3 .

Reaction set 1



The above cycle can be generalized for other precursors like methane (CH_4) and nonmethane hydrocarbons (NMHCs) as well. The production efficiency of O_3 has been observed to depend on several meteorological parameters such as solar radiation flux and temperature. In general, O_3 mixing ratio will increase when incoming solar ultraviolet (UV) flux reaches a maximum, clouds are few and levels of precursors are optimum (determined by VOCs/ NO_x ratio). The level of NO_2 which represents a major part of NO_x is critical for determining the O_3 production efficiency through the formation of $O(^3P)$ atom. Subsequently, $O(^3P)$ combines with molecular oxygen (O_2) leading to the formation of O_3 . On the other hand, excessive conversion of NO from NO_2 can directly react with O_3 , leading to loss of ambient O_3 by the following titration reaction.

Reaction set 2



In addition to the direct effect of UV radiation on O_3 production, emissions of some O_3 precursors are temperature-dependent and peak during the mid-summer in the tropical region. For example, the biogenic or natural emissions of hydrocarbons are particularly sensitive to temperature and follow the seasonal cycles of controlling

*For correspondence. (e-mail: lokesh@prl.res.in)

meteorological parameters². Variations in the surface-level temperature can strongly influence the kinetics of reactions leading to the production of O₃, and boundary layer processes through mixing with O₃-rich free tropospheric air mass³.

It is important to mention that the impact of meteorological parameters on O₃ levels has been reported in several studies⁴. For example, the episodes of photochemical smog (in which O₃ is an important constituent) are usually associated with high-pressure system. Consequently, the surface-level O₃ concentrations show strong seasonal variations partly due to seasonal changes in meteorological parameters.

The statistical methods for air-quality prediction have been used in many studies⁵. Most of these methods include multiple linear regression analysis^{6–8}. However, the linear regression models have been found to be inadequate to simulate the complex relationship between O₃ and meteorology. The linear regression approach is applied based, in part, on the strong correlation between maxima in surface O₃ and temperature. However, it is difficult to understand and visualize the real processes without the comprehensive photochemical modelling⁹.

The importance of photolysis in the formation of O₃ provides a direct link between O₃ and temperature with respect to time of the year. The temperature-dependent photochemical rate constants also provide a link between O₃ and temperature^{10,11}.

The effect of temperature on O₃ has been observed in different regions of the world. Several studies have explored the above-mentioned aspect, especially over the tropical stations, where measurement data are sparse^{12,13}. There is a need to understand the role of local meteorological factors in the photochemical production of O₃. Understanding the relation of daily maximum in O₃ (O_{3max} hereafter) with maximum in temperature (T_{max} hereafter) could be used to forecast O₃ levels. Such studies of O₃ in relation with other meteorological parameters (predictors) are also important to forecast the O₃ episode events. In this communication, we have studied the seasonal dependencies of O_{3max} on T_{max} using the surface observation data at an urban site, i.e. Pune, India during the period 2003–04. Also, the dependence of O_{3max} on minimum of NO_x (NO_{xmin}) has been studied to assess the role of the chemical mechanism controlling O_{3max} levels.

The observational site is situated at the northwest region of Pune city (18.4°N, 73.8°E). Pune is an industrialized city; however, the observational site at the Indian Institute of Tropical Meteorology (IITM) campus is located at distance of about 20–25 km from the main industrial zone. Some sugar factories are located to the northeast of the site. In the winter season, the wind pattern is northeasterly which can transport the pollutants, including the ozone precursor to the site. The measurement site is surrounded by hills, while moderate commuter

traffic is observed on the nearby roads, which is about 200 m from the site¹⁴. From early May to September/October each year, when the inter-tropical convergence zone (ITCZ) moves northward across India, cleaner marine air masses from the Arabian Sea and the Indian Ocean dominate at Pune. The polluted continental air masses prevail when the ITCZ moves back southward in September and October. In the winter season, the wind flow is mostly westerly and northwesterly winds¹⁵. At this site, the morning and evening rush hours (period of heavy vehicular traffic) coincide with the increasing and decreasing heights of boundary layer depth respectively. Therefore, the interplay between the planetary boundary layer (PBL) depth and local emission defines the magnitude and duration of rush-hour peaks observed in the levels of primary pollutants. On the other hand, the local biomass burning emissions and long-range transport of pollutants also play an important role in the distribution of trace gases.

The surface-level O₃ is measured using an on-line analyser (O₃42M, Environment S.A., French-make) based on absorption of UV radiation at 253.7 nm. The analyser automatically incorporates the corrections due to changes in temperature and pressure in the absorption cell. The minimum detection limit of the analyser is 1 ppbv with noise of about 0.5 ppbv, for 10 s response time. The mixing ratios of O₃ are always well above 5 ppbv for ambient measurements at this site, which gives a large signal-to-noise ratio. To cross-check the data accuracy, an automatic cycle of zero reference is generated after every 8 h. The absolute accuracy of these instruments is reported to be about 5% (ref. 16). The data resolution of 1 min to 24 h can be stored in the memory available in the instrument. More details are available at the website: <http://www.environnement-sa.com>.

The mixing ratio of NO_x is measured with the analyser (APNA 365, Horiba, Japan) based on chemiluminescence technique. The inter-comparison of these measurements with more specific techniques suggests that all surface converters that are sufficiently robust to convert NO₂ to NO and also convert other reactive nitrogen oxide species, such as PAN to NO, thereby causing an interference in the NO_x measurements^{17,18}. The magnitude of this interference may vary significantly with location and material used for conversion of NO₂ to NO; molybdenum in the present case. It is generally believed that this interference is the smallest for urban/semi-urban measurements, where NO₂ and NO comprise of a major fraction of oxides of nitrogen and hence measures NO_x, provided all the values are viewed as upper limits to their true values¹⁹. The quality of measured data has been maintained by regular zero and span calibrations. For span calibration, a known amount of NO₂ gas was generated by a calibrator using a NO₂ permeation tube. The multipoint calibration, between 0 and 100 ppbv (steps of ~10 ppbv), of NO_x, was performed on regular basis. However, the

lack of zero check facility (inbuilt), unlike for the ozone analyser, is major disadvantage with the NO_x measurement. Therefore, external zeroing and calibration were performed by supplying zero air (a pure mixture of N₂ and O₂ gases) and calibration mixture respectively. The zeroing and calibration checks were performed every week; however, we needed to change the calibration factors in a period of 45–60 days. The minimum detection limit of the analyser is 100 pptv, providing large signal-to-noise ratio as ambient measurements are always higher than 1000 pptv (ref. 14). Further details of the instrument are described in the website: <http://www.horiba.com/>.

In the present work, we have used the daily data of O₃, NO_x as well as temperature data for the period June 2003–May 2004. The surface temperature data were regularly recorded from a weather station near the measurement site (IMD Daily Weather Report 2003–04). In this study, analyses of data have been classified in view of two different aspects of the study. First, the correlation study of O₃ with temperature, which is addressed by investigating the relation between daily O_{3,max} and T_{max}. The second aspect is based on the chemical process for which relation between O_{3,max} and NO_{x,min} has been studied. The concept of studying O_{3,max} in relation with a meteorological parameter (T_{max}) is to understand the role of local meteorology, responsible for the occurrences of O_{3,max} in an urban environment.

Figure 1 shows the time-series variations of daily O_{3,max} and T_{max} for different seasons. Typically, seasons are classified as follows: monsoon (June–September), post-monsoon (October–December), winter (January–February) and pre-monsoon (summer: March–May) over the Indian subcontinent (http://www.imdpune.gov.in/weather_forecasting/glossary.pdf). Figure 1*a* shows the variations of O_{3,max} and T_{max} during the monsoon season. The mean values of O_{3,max} and T_{max} are 25 ± 11 ppbv and 29 ± 3°C respectively, during the monsoon season. In this season, the highest values of O_{3,max} and T_{max} are 67 ppbv and 39°C respectively.

Table 1 provides statistical parameters derived from the linear fits between O_{3,max} and T_{max} for different seasons. It is to be noted that terms like ‘linear fit’, ‘R²’, ‘correlation coefficient’, and similar expressions generally refer to the parameters derived from the linear regression analysis/fit. Although O_{3,max} tends to slightly increase with T_{max}, the linear fit shows moderate correlation in the monsoon season (Figure 2*a*). During this season, the estimated rate of increase (ΔO_{3,max}/ΔT_{max}) is lowest, i.e. 1.31 ppbv °C⁻¹. Solar radiation plays a vital role in controlling the levels of O₃ and temperature. More importantly, reduced emissions due to negligible presence of open biomass burning and transport of cleaner marine air result in lower levels of various precursor gases required for O₃ production^{20,21}. Due to insufficient levels of O₃ precursors and solar radiation intensity, the level and variation of O_{3,max} and T_{max} are relatively less compared to

other seasons. In addition, particularly applicable for low NO_x condition during monsoon, the following reaction with HO₂ radicals may account for major loss of ozone²².

Reaction set 3

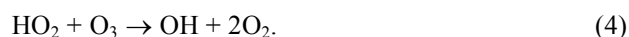
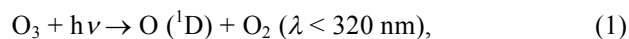


Figure 1*b* shows the variations of O_{3,max} and T_{max} during the post-monsoon season. The mean values of O_{3,max} and T_{max} are 73 ± 17 ppbv and 30.5 ± 2°C respectively, during the postmonsoon season. In this season, the ranges of O_{3,max} and T_{max} are 18–123 ppbv and 26–33°C respectively. The values of O_{3,max} tend to increase with higher T_{max} and show somewhat poor correlation (r² = 0.20) compared to the monsoon season (Figure 2*b*). In the post-monsoon season, the estimated rate of increase (ΔO_{3,max}/ΔT_{max}) is 3.56 ppbv °C⁻¹. The transition from southwesterly to northeasterly wind flow seems to be a major reason for the large variations of O₃ and temperature. In the later part of this season, the photochemical production and transport of continental air lead to increase in O₃. Therefore, onset of open biomass burning and transport of polluted continental air result in higher levels of various precursor gases required for O₃ production in the later part of the post-monsoon season.

Figure 1*c* shows the time-series variations of daily O_{3,max} and T_{max} during the winter season. The mean values of daily O_{3,max} and T_{max} are 62 ± 28 ppbv and 30 ± 3°C, respectively. The values of both daily O_{3,max} and T_{max} show large variations in the range 20–99 ppbv and 25–36°C respectively. Table 1 shows moderate correlation (r² = 0.54) between O_{3,max} and T_{max} for the winter season. One of the possible mechanisms for the observed high O₃ may be breaking of the PBL inversion caused by higher afternoon temperature and downdraft of O₃-rich air from the free troposphere²³. The mixing ratio of O_{3,max} increases at the highest rate of 7.1 ppbv °C⁻¹, which is significantly high compared to monsoon and postmonsoon seasons. In the later part of the winter season, the high baseline value could also be caused by the transport of continental O₃-rich air from the NW–NE wind directions²⁴. On the other hand, some studies have reported that the increased level of O₃ will tend to increase the temperature due to greenhouse effect²⁵.

Figure 1*d* shows the variations of daily O_{3,max} and T_{max} for the pre-monsoon season. In this season, the mean values of daily O_{3,max} and T_{max} are 66 ± 23 ppbv and 37 ± 2°C respectively. The highest value of daily O_{3,max} and T_{max} are 100 ppbv and 41°C respectively. The increasing trend of O_{3,max} with temperature is observed up to 37°C,

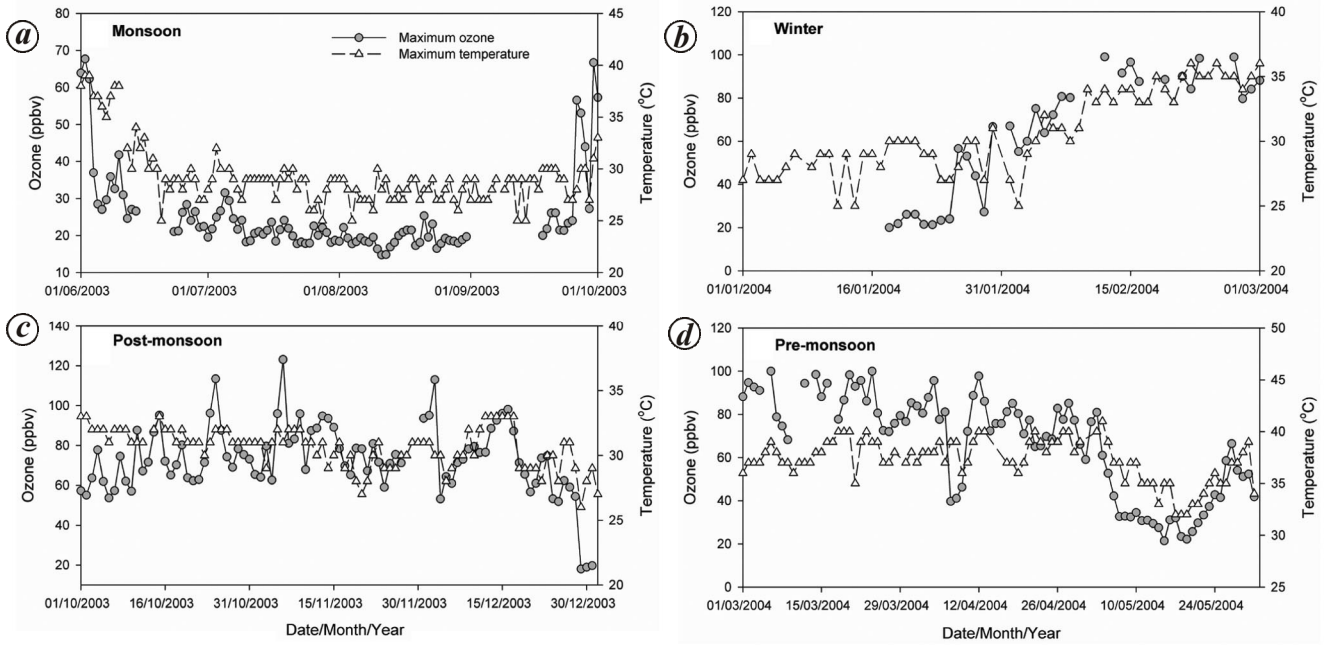


Figure 1 a–d. Time series of daily maximum values of ozone (O_{3max}) and temperature (T_{max}) during different seasons at Pune, India.

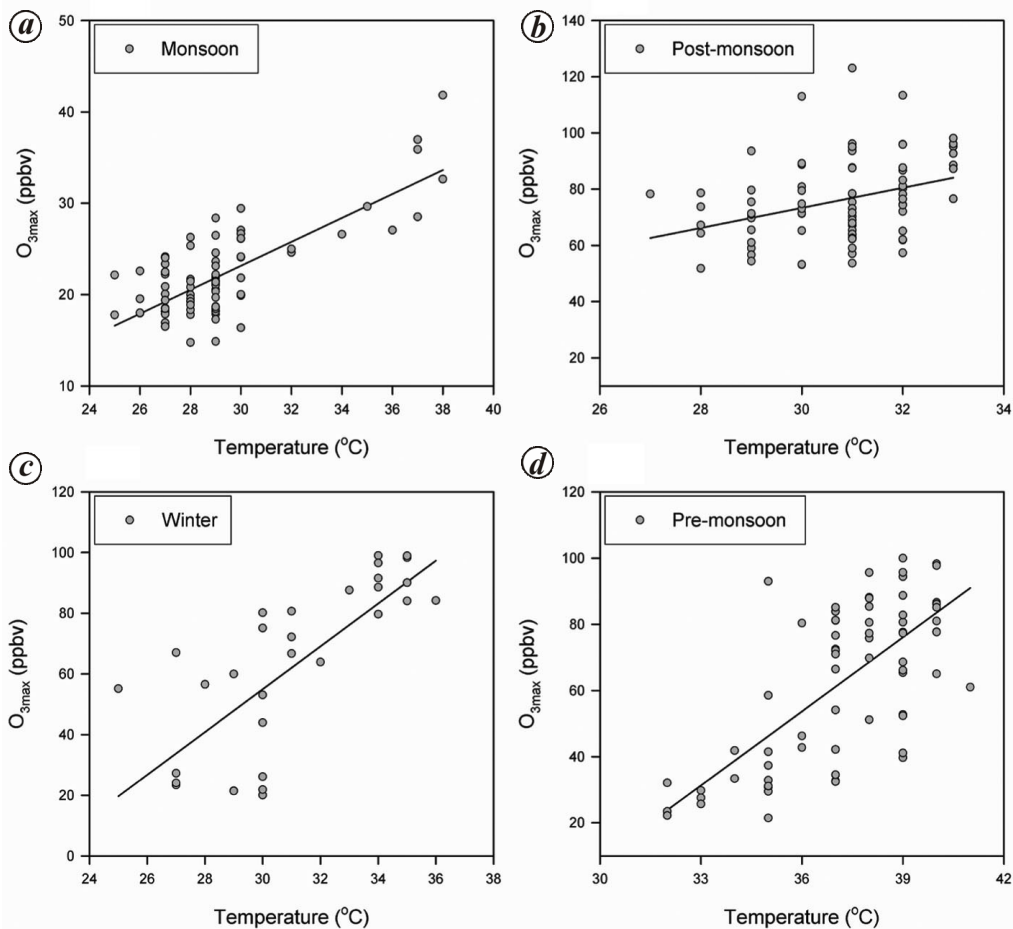


Figure 2 a–d. Scatter plots between O_{3max} and T_{max} for four different seasons of measurements at Pune, India.

after which a decrease in $O_{3\max}$ level can be noticed. In this season, the values of T_{\max} often exceed the level of 37°C at this site. The results are consistent with those of Neuman *et al.*²³, who have reported that the mixing ratios of O_3 remain low at low temperature and increase with increasing temperature, but for temperature in excess of 35°C , there is little response. In the pre-season, the estimated rate of increase ($\Delta O_{3\max}/\Delta T_{\max}$) is $7.5 \text{ ppbv } ^{\circ}\text{C}^{-1}$, which is almost the same as observed for the winter season. A study over southern USA reports that the number of O_3 molecules produced per NO_y (NO_x + all of its reservoir species) molecule increases with temperature between 22°C and 33°C (ref. 26). The lower levels of precursors during pre-monsoon can be due to strong surface heating and hence convective ventilation leading to reduction in O_3 production rate compared to winter season¹⁴. The severe cyclonic storms in the Arabian Sea and the heavy rainfall associated with it would have resulted in the decrease of O_3 and temperature²⁷. The relations

between $O_{3\max}$ and T_{\max} can also be impacted by other factors than just those affecting the local loss and production of O_3 . For example, long-range transport of different air masses having different O_3 concentrations from the different regions. In particular, the annual emissions of O_3 precursors increase due to the highest activities of biomass burning during this season¹⁴.

The simultaneous measurements of other pollutants provide an opportunity to examine the relationship of O_3 with its precursors and tracers of anthropogenic pollutants^{28,29}. At the receptor site, CO , NO_x and total NMHCs were continuously measured in conjunction with O_3 . Detailed analyses of this dataset are given elsewhere¹⁴. It has been observed that the association between primary pollutants (directly emitted from the sources) and temperature is weak or insignificant, as these are mainly emitted from the anthropogenic sources. Whereas the secondary pollutants (mostly formed photochemically) are positively correlated with temperature. Figure 3 shows the vertical bar plots of correlation coefficients between daily $O_{3\max}$ and T_{\max} (Figure 3a) and daily $O_{3\max}$ and $\text{NO}_{x\min}$ (Figure 3b) for the different months of the period 2003–04. It can be seen in Figure 3a that tight correlation between $O_{3\max}$ and T_{\max} is observed during most of the months. In other words, the positive correlation between $O_{3\max}$ and $\text{NO}_{x\min}$ indicates a significant role of the reduced loss of O_3 due to less NO titration (reaction set 2). Overall, the results presented in this study support the views that the role of local meteorology should not be disregarded to interpret the variation of ambient level O_3 in urban regions^{30,31}.

This study is based on statistical analysis of surface-level observations of daily maxima of ozone ($O_{3\max}$) and ambient air temperature (T_{\max}) at an urban site, i.e. Pune, India during 2003–04. Except for the monsoon season, the time-series variation of maximum ozone follows the variation of daily maximum temperature. The linear regression fits between daily maxima in O_3 and temperature show positive relations; however, with poor and excellent correlations during monsoon and winter seasons respectively. The ranges of daily $O_{3\max}$ are 14.7–67.7, 18–123, 20–99 and 21.5–100 ppbv during monsoon, post-monsoon, winter and pre-monsoon seasons respectively. On the other hand, the ranges of daily T_{\max} are $25\text{--}39^{\circ}\text{C}$, $26\text{--}33^{\circ}\text{C}$, $25\text{--}36^{\circ}\text{C}$ and $32\text{--}41^{\circ}\text{C}$ during monsoon, post-monsoon, winter and premonsoon seasons respectively. In order to understand the role of photochemical processes, particularly titration due to NO_x , we have studied the relation between maximum O_3 and minimum NO_x mixing ratios. However, analysis is presented based on the relation with temperature only. The present study highlights the role of local meteorology in controlling the ambient levels of O_3 in an urban environment.

Table 1. Parameters derived from the linear fits between daily $O_{3\max}$ and T_{\max} for different seasons

Season	r^2	Slope (ppbv $^{\circ}\text{C}^{-1}$)
Monsoon	0.57	1.31
Post-monsoon	0.20	3.56
Winter	0.54	7.1
Pre-monsoon	0.50	7.5

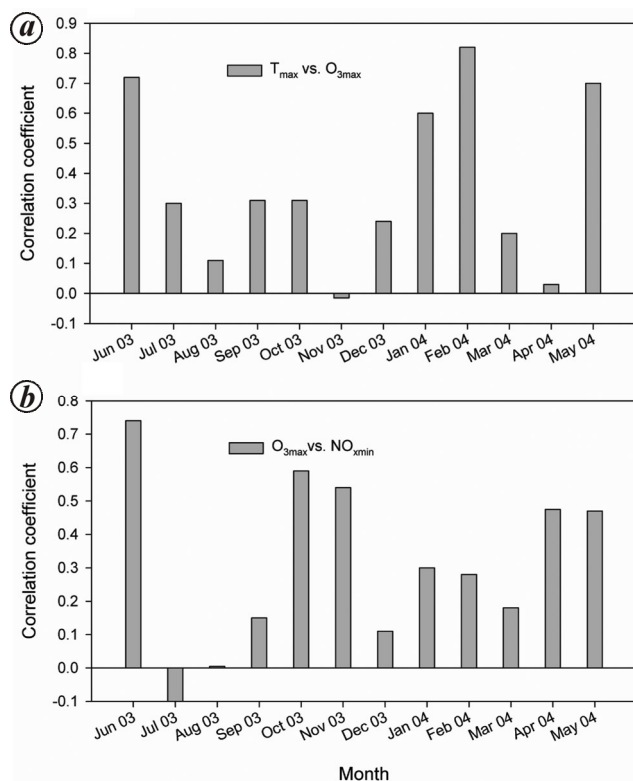


Figure 3. Correlation coefficients between daily (a) $O_{3\max}$ and T_{\max} and (b) $O_{3\max}$ and $\text{NO}_{x\min}$ for different months during 2003–04 at Pune.

1. Sahu, L. K., Volatile organic compounds and their measurements in the troposphere. *Curr. Sci.*, 2012, **102**(10), 1645–1649.

2. Goldstein, A. H., Goulden, M. L., Munger, J. W., Wofsy, S. C. and Geron, C. D., Seasonal course of isoprene emissions from a mid-latitude deciduous forest. *J. Geophys. Res. – Atmosph.*, 1998, **103**, 31045–31056.
3. Wang, T., Lam, K. S., Lee, A. S. Y., Pang, S. W. and Tsui, W. S., Meteorological and chemical characteristics of the photochemical ozone episodes observed at cape d'aguilar in Hong Kong. *J. Appl. Meteorol.*, 1998, **37**, 1167–1178.
4. Colbeck, I. and Mackenzie, A. R., Air pollution by photochemical oxidants. *Air Qual. Monogr.*, 1994, **1**, 376.
5. Robeson, S. M. and Steyn, D. G., Evaluation and comparison of statistical forecast models for daily maximum ozone concentrations. *Atmos. Environ. B*, 1990, **24**, 303–312.
6. Clark, T. L. and Karl, T. R., Application of prognostic meteorological variables to forecasts of daily maximum one-hour ozone concentrations in the northeastern United States. *J. Appl. Meteorol.*, 1982, **21**, 1662–1671.
7. Feister, U. and Balzer, K., Surface ozone and meteorological predictors on a subregional scale. *Atmos. Environ. A*, 1990, **25**, 1791–1800.
8. Ryan, W. F., Forecasting severe ozone episodes in the Baltimore metropolitan area. *Atmos. Environ.*, 1995, **29**, 2387–2398.
9. Beaney, G. and Gough, W. A., The influence of tropospheric ozone on the air temperature of the city of Toronto, Canada. *Atmos. Environ.*, 2002, **36**, 2319–2325.
10. Sillman, S., Logan, J. A. and Wofsy, S. C., The sensitivity of ozone to nitrogen oxides and hydrocarbons in regional ozone episodes. *J. Geophys. Res.*, 1990, **95**, 1837–1851.
11. Cardelino, C. A. and Chameides, W. L., Natural hydrocarbons, urbanization, and urban ozone. *J. Geophys. Res.*, 1990, **95**, 13971–13979.
12. Elampari, K. and Chithambarhanu, T., Diurnal and seasonal variations in surface ozone levels at tropical semi-urban site, Nagercoil, India, and relationships with meteorological conditions. *Int. J. Sci. Technol.*, 2011, **1**, 80–88.
13. Bhuyan, P. K., Bharali, C., Pathak, B. and Kalita, G., The role of precursor gases and meteorology on temporal evolution of O₃ at a tropical location in northeast India. *Environ. Sci. Pollut. Res.*, 2014, **21**, 6696e6713; <http://dx.doi.org/10.1007/s11356-014-2587-3>.
14. Beig, G., Gunthe, S. and Jadhav, D. B., Behavior of surface ozone with its precursors on a diurnal scale at the semi-urban site in India. *J. Atmos. Chem.*, 2007, **57**.
15. Asnani, G. C., Inter tropical convergence zone. *Trop. Meteorol. IITM, Pune 8*, 1993, vol. 1, p. 1202.
16. Kleinman, L. *et al.*, Ozone formation at a rural site in the southeastern united-states. *J. Geophys. Res.-Atmosp.*, 1994, **99**, 3469–3482.
17. Winer, A. M., Peters, J. W., Smith, J. P. and Pitts, J. N., Response of commercial chemiluminescent NO–NO₂ analyzers to other nitrogen-containing compounds. *Environ. Sci. Technol.*, 1974, **8**, 1118–1121.
18. Singh, H. B. *et al.*, Relationship between peroxyacetyl nitrate and nitrogen-oxides in the clean troposphere. *Nature*, 1985, **318**, 347–349.
19. Chameides, W. L. *et al.*, Ozone precursor relationships in the ambient atmosphere. *J. Geophys. Res.-Atmosp.*, 1992, **97**, 6037–6055.
20. Sahu, L. K. and Lal, S., Distribution of C₂–C₅ NMHCs and related trace gases at a tropical urban site in India. *Atmos. Environ.*, 2006, **40**, 880–891.
21. Lelieveld, J. and Crutzen, P. J., Influences of cloud photochemical processes on tropospheric ozone. *Nature*, 1990, **343**, 227–233.
22. Parrish, D. D. *et al.*, Background ozone and anthropogenic ozone enhancement at Niwot Ridge, Colorado. *J. Atmos. Chem.*, 1986, **4**, 63–80.
23. Neuman, J. A. *et al.*, Observations of ozone transport from the free troposphere to the Los Angeles basin. *J. Geophys. Res.*, 2012, **117**, D00V09; <http://dx.doi.org/10.1029/2011JD016919>.
24. Beig, G. and Brasseur, G. P., Influence of anthropogenic emissions on tropospheric ozone and its precursors over the Indian tropical region during a monsoon. *Geophys. Res. Lett.*, 2006, **33**, L07808; doi: 10.1029/2005GL024949.
25. Monks, P. S. *et al.*, Atmospheric composition change – global and regional air quality. *Atmos. Environ.*, 2009, **43**, 5268–5350.
26. Olszyna, K. J., Luria, M. and Meagher, J. F., The correlation of temperature and rural ozone levels in southeastern USA. *Atmos. Environ.*, 1997, **31**, 3011–3022.
27. Das, S. S. *et al.*, Influence of tropical cyclones on tropospheric ozone: possible implication. *Atmos. Chem. Phys. Dis.*, 2015, **15**(13), 19305–19323.
28. Fischer, H., *et al.*, Ozone production and trace gas correlations during the June 2000 minatroc intensive measurement campaign at Mt. Cimone. *Atmos. Chem. Phys.*, 2003, **3**, 725–738.
29. Lal, S., Sahu, L. K., Venkataramani, S., Rajesh, T. A. and Modh, K. S., Distributions of O₃, CO and NMHCs over the rural sites in central India. *J. Atmos. Chem.*, 2008, **61**(1), 73–84; doi: 10.1007/s10874-008-9115-0.
30. Sahu, L. K. and Lal, S., Characterization of C₂–C₄ NMHCs distributions at a high altitude tropical site in India. *J. Atmos. Chem.*, 2006, **54**(2), 161–175; doi: 10.1007/s10874-006-9023-0.
31. Sahu, L. K. and Saxena, P., High time and mass resolved PTR-TOF-MS measurements of VOCs at an urban site of India during winter: role of anthropogenic, biomass burning, biogenic and photochemical sources. *Atmos. Res.*, 2015, **164–165**, 84–94; ISSN 0169-8095, <http://dx.doi.org/10.1016/j.atmosres.2015.04.021>.

Received 26 March 2015; revised accepted 6 January 2016

doi: 10.18520/cs/v110/i10/1994-1999

Diversity of cyanobacteria in biological crusts on arid soils in the Eastern region of India and their molecular phylogeny

Dhanesh Kumar^{1,2}, Petr Kaštanek² and Siba P. Adhikary^{1,3,*}

¹Department of Biotechnology, Siksha-Bhavana, Visva-Bharati, Santiniketan 731 235, India

²Faculty of Food and Biochemical Technology, Institute of Chemical Technology, Prague-6, Czech Republic

³Fakir Mohan University, Vyasa Vihar, Nuapadhi, Balasore 756 020, India

The biological crusts on lateritic soils, red soils and mine-waste burdened soils in the eastern region of India covering a transect of about 800 km were principally composed of sheathed cyanobacteria of the genera *Scytonema*, *Tolypothrix* and *Lyngbya* along with few other species of *Cylindrospermum*, *Nostoc*, *Calothrix* and *Fischerella*. Molecular phylogeny based on 16S rRNA gene sequence of these cyanobacteria along with those occurring in different habitats of four

*For correspondence. (e-mail: adhikarysp@gmail.com)